Frontiers in Bioscience Landmark

Front. Biosci. (Landmark Ed) **2026**; 31(1): 46525
https://doi.org/10.31083/FBL46525

Original Research

Neuroprotective Effects of the SIRT3/AMPK Axis in Experimental Glaucoma

Feng Chen[1,2], Ying Yu[2], Xiaoxiao Cai[2], Xiaohe Lu[1,*]

[1]Department of Ophthalmology, Zhujiang Hospital of Southern Medical University (The Second School of Clinical Medicine), 510280 Guangzhou, Guangdong, China
[2]Department of Ophthalmology, Guangzhou Women and Children's Medical Center, Guangzhou Medical University, 510623 Guangzhou, Guangdong, China
*Correspondence: luxh63@163.com (Xiaohe Lu)
Academic Editors: Luigi Donato and Dario Rusciano
Submitted: 12 September 2025 Revised: 6 November 2025 Accepted: 17 November 2025 Published: 14 January 2026

Abstract

Background: Glaucoma is a major cause of irreversible blindness, characterized by the progressive degeneration of retinal ganglion cells (RGCs), with oxidative stress and apoptosis playing central roles in its pathogenesis. Sirtuin 3 (SIRT3) has demonstrated antioxidant and anti-apoptotic effects in various neurodegenerative diseases; however, its precise role in glaucoma remains unclear. This study aimed to elucidate the neuroprotective function and mechanistic basis of the SIRT3/AMP-activated protein kinase (AMPK) axis in glaucoma. **Methods**: A rat model of chronic ocular hypertension (COH) was generated using cross-linked hydrogel injection, while an N-methyl-D-aspartate (NMDA)-induced RGC injury model was developed *in vitro*. SIRT3 overexpression was achieved using adeno-associated virus (AAV) transfection, either alone or combined with the AMPK inhibitor Compound C. Functional and molecular analyses were performed, including intraocular pressure (IOP) measurement, hematoxylin–eosin (H&E) staining, Terminal deoxynucleotidyl transferase dUTP nick end labeling (TUNEL) assay, immunofluorescence, Cell Counting Kit-8 (CCK-8) cell viability assay, flow cytometry, Quantitative real-time PCR (qRT-PCR), and western blotting. **Results**: In the COH model, both SIRT3 expression and the p-AMPK/AMPK ratio were significantly reduced at weeks 2, 4, and 6 ($p < 0.05$). Overexpression of SIRT3 lowered IOP, preserved retinal thickness, and decreased the number of TUNEL-positive cells ($p < 0.001$), while Compound C partially reversed these effects ($p < 0.05$). In addition, SIRT3 overexpression markedly educed reactive oxygen species (ROS) accumulation ($p < 0.001$) and restored the p-AMPK/AMPK ratio ($p < 0.001$), both of which were partially inhibited by Compound C. In NMDA-induced RGCs, SIRT3 overexpression significantly increased SIRT3 mRNA levels ($p < 0.01$), enhanced cell viability ($p < 0.001$), and suppressed apoptosis ($p < 0.001$), with these effects attenuated by Compound C ($p < 0.01$). The reduction of ROS and activation of AMPK by SIRT3 in this model were also partly reversed by AMPK inhibition ($p < 0.01$). **Conclusion**: This study provides the first comprehensive *in vivo* and *in vitro* evidence in glaucoma models that SIRT3 confers neuroprotection in experimental glaucoma, primarily through activation of the AMPK signaling pathway. These findings identify the SIRT3/AMPK axis as a novel mechanistic target and suggest a promising therapeutic strategy for IOP-independent neuroprotection in glaucoma.

Keywords: Sirtuin 3; AMP-activated protein kinases; glaucoma; oxidative stress; apoptosis; retinal ganglion cells; neuroprotection

1. Introduction

Glaucoma is a major cause of blindness worldwide, affecting over 76 million people in 2020, with the number expected to rise to 111.8 million by 2040, particularly impacting aging populations in the Asia-Pacific region [1]. This neurodegenerative disease is characterized by the progressive loss of retinal ganglion cells (RGCs) and optic nerve damage, resulting in irreversible visual field defects and blindness [2]. Current therapeutic strategies primarily aim to lower intraocular pressure (IOP), which can slow but not halt disease progression. However, many patients continue to experience progressive vision loss despite achieving target IOP levels, highlighting the urgent need for alternative approaches that preserve RGC integrity and function [3].

Mounting evidence has identified oxidative stress and apoptosis as key pathological mechanisms underlying glaucomatous neurodegeneration. Chronic ocular hypertension (COH) and excitotoxic stimuli promote excessive production of reactive oxygen species (ROS), disrupt mitochondrial respiration, and activate caspase-dependent apoptotic pathways. These events impair axonal transport and synaptic communication, ultimately resulting in irreversible neuronal death [4–6]. Given the critical role of oxidative stress in RGC injury, modulating redox homeostasis and mitochondrial function has emerged as a promising avenue for neuroprotection in glaucoma [7].

Sirtuin 3 (SIRT3), a mitochondrial NAD^+-dependent deacetylase, is a central regulator of mitochondrial metabolism, oxidative defense, and cellular stress adaptation [8]. By deacetylating enzymes in the electron transport chain and antioxidant systems such as superoxide dismutase 2, SIRT3 reduces ROS accumulation, stabilizes mitochondrial membrane potential, and preserves bioener-

getic homeostasis [9]. While SIRT3 has been shown to exert neuroprotective effects in conditions including cerebral ischemia, Parkinson's disease, and Alzheimer's disease [10,11], its role in RGCs under glaucomatous stress remains poorly characterized. To date, no study has specifically examined SIRT3 expression dynamics in RGCs or assessed the impact of SIRT3 deletion on RGC survival following glaucomatous injury, underscoring the novelty of exploring the SIRT3/AMP-activated protein kinase (AMPK) axis in this context.

Among the seven mammalian sirtuins (SIRT1–SIRT7), SIRT3 is the primary mitochondrial isoform, whereas other members such as SIRT1 and SIRT2 are mainly localized in the nucleus or cytoplasm [12]. This unique mitochondrial localization enables SIRT3 to directly regulate oxidative phosphorylation, reactive oxygen species (ROS) detoxification, and mitochondrial energy metabolism, thereby distinguishing it from other SIRTs that primarily modulate nuclear transcriptional or cytosolic signaling processes [13]. Previous studies have largely focused on SIRT1 and SIRT6 in the retina, reporting their involvement in autophagy and inflammatory regulation, respectively, whereas the contribution of mitochondrial SIRT3 to glaucomatous neurodegeneration remains largely unexplored [14,15]. Given its essential role in maintaining mitochondrial redox homeostasis and preventing neuronal apoptosis under oxidative stress, investigating SIRT3 may provide critical insights into mitochondrial dysfunction during glaucoma progression [16].

In addition to SIRT3, multiple oxidative stress regulators—including Nuclear factor erythroid 2–related factor 2 (Nrf2), Peroxisome proliferator–activated receptor gamma coactivator 1-alpha (PGC-1α), and superoxide dismutase (SOD)—have been implicated in glaucoma pathophysiology. Nevertheless, SIRT3 lies upstream of many of these antioxidant pathways, acting as a metabolic hub that coordinates Nrf2 activation, Manganese superoxide dismutase (MnSOD) deacetylation, and AMPK-dependent mitochondrial biogenesis [17,18]. Thus, targeting the SIRT3/AMPK axis provides an integrative approach to restore mitochondrial function and redox homeostasis, potentially yielding broader neuroprotective benefits than single-pathway modulation. Beyond its experimental relevance, SIRT3 activation also carries translational potential, as several sirtuin activators—such as resveratrol and nicotinamide—are currently being evaluated in clinical trials for neurodegenerative diseases, supporting the feasibility of modulating sirtuin pathways for glaucoma therapy [19,20]. This mechanistic framework highlights the added value of the present study, which systematically evaluates the SIRT3/AMPK interaction as a distinct and convergent node in oxidative stress regulation during glaucomatous injury.

One of the key downstream effector of SIRT3 is AMP-activated protein kinase (AMPK), a master regulator of intracellular energy status that modulates oxidative stress responses, mitochondrial biogenesis, and autophagy [21]. Activation of AMPK has been linked to reduced oxidative damage and improved neuronal survival in various central nervous system pathologies [22]. However, the potential cross-talk between SIRT3 and AMPK in the glaucomatous retina—particularly in regulation of oxidative stress and apoptosis—remains poorly understood. Clarifying this interaction could provide valuable insights into novel, mechanism-based strategies for glaucoma management beyond IOP reduction.

Therefore, the present study aimed to investigate whether SIRT3 overexpression confers neuroprotection in glaucoma-associated injury, using both an *in vivo* chronic ocular hypertension (COH) rat model and an *in vitro* N-methyl-D-aspartate (NMDA)-induced retinal ganglion cell (RGC) injury model. Furthermore, we examined whether pharmacological inhibition of AMPK would attenuate the neuroprotective effects of SIRT3, thereby testing the hypothesis that SIRT3-mediated protection operates, at least in part, through AMPK activation. By elucidating this mechanism, our study provides novel insight into the mitochondrial regulation of oxidative stress in glaucoma and identifies the SIRT3/AMPK axis as a potential therapeutic target distinct from previously studied sirtuin pathways.

2. Materials and Methods

2.1 Animals and Grouping Design

Male Sprague–Dawley (SD) rats (200–220 g, 6–8 weeks) were obtained from the Institute of Laboratory Animal Sciences, Chinese Academy of Medical Sciences (Beijing, China). All animal procedures were approved by the Animal Ethics Committee of Guangzhou Medical University (Approval No. KTDW-2024-00947) and conducted in accordance with institutional and national guidelines. Animals were housed under standard laboratory conditions (22 $\pm$ 2 °C, 12-h light/dark cycle) with free access to food and water.

Chronic ocular hypertension (COH) was induced in the right eye by anterior chamber injection of a freshly prepared cross-linked hydrogel composed of HyStem® (thiol-modified carboxymethyl hyaluronic acid; Catalog No. HYS020) and its corresponding Extralink® crosslinker (thiol-reactive polyethylene glycol diacrylate; supplied within the HyStem® kit; both from Sigma-Aldrich, St. Louis, MO, USA) at a 4:1 volume ratio. A total of 7 µL of hydrogel was slowly injected using a microsyringe with a 33-gauge needle, and the needle was withdrawn gradually over 30 seconds to prevent leakage. Following injection, 0.3% ofloxacin ointment (Catalog No. 070102; Shenyang Xingqi Pharmaceutical Co., Ltd., Shenyang, China) was applied to the cornea to prevent infection [23,24].

All surgical procedures were performed under general anesthesia induced by isoflurane inhalation (1–3% in oxygen). Adequate anesthetic depth was confirmed by the

absence of corneal and pedal reflexes before the start of surgery. During the procedure, animals were placed on a heating pad to maintain body temperature at 37 °C, and anesthesia was continuously maintained with isoflurane inhalation throughout the operation. At the end of the surgery, 0.3% ofloxacin ophthalmic ointment was applied to prevent infection.

The *in vivo* study comprised two designs (n = 6 per group):

(1) Time-course analysis of SIRT3 expression in COH: Control group: Phosphate-buffered saline (PBS) administered into the anterior chamber of the right eye; COH group: Hydrogel administration as described above. IOP and retinal samples were collected at weeks 0, 2, 4, and 6.

(2) Functional analysis of the SIRT3/AMPK axis in COH: (a) Control and COH: As described above; (b) COH+AAV-NC: Intravitreal injection of 5 µL AAV-NC (5×10^9 viral particles; customized product without a universal catalog number, GeneChem, Shanghai, China) 48 h before COH induction. Injection was performed over 60 s, keeping the needle in position for 1 min before withdrawal; (c) COH+AAV-SIRT3: Same procedure as above, replacing AAV-NC with AAV-SIRT3 (5×10^9 viral particles; customized product without a universal catalog number, GeneChem, Shanghai, China); (d) COH+AAV-SIRT3 + Compound C: AAV-SIRT3 injection as above, with additional intravitreal administration of Compound C (AMPK inhibitor; 10 nmol; Catalog No. 171261, MedChemExpress, USA) on the day of COH induction [23,24]. All treatments were performed in the same eye, and contralateral eyes served as internal controls when appropriate.

2.2 Cell Culture and Experimental Groups

Primary RGCswere obtained from neonatal SD rats (postnatal day 1–3) provided by the Institute of Laboratory Animal Sciences, Chinese Academy of Medical Sciences (Beijing, China). Neonatal rats were euthanized by intraperitoneal injection of sodium pentobarbital (150 mg/kg), administered by trained personnel to ensure rapid induction of deep anesthesia and subsequent cessation of cardiac and respiratory activity. Death was verified by the absence of vital signs. All procedures were approved by the Ethics Committee of Guangzhou Medical University (Approval No. KTDW-2024-00947) and carried out in accordance with the ARVO Statement for the Use of Animals in Ophthalmic and Vision Research.

Retinas were rapidly dissected under a stereomicroscope (SZX7, Olympus Corporation, Tokyo, Japan) in ice-cold Hanks' balanced salt solution (HBSS; Catalog No. 14175095, Thermo Fisher Scientific, Waltham, MA, USA), enzymatically digested with papain (Catalog No. LS003126, Worthington Biochemical Corporation, Lakewood, NJ, USA) prior to mechanical dissociation. Primary RGCs underwent purification through a two-step immunopanning technique and were maintained on poly-D-lysine–coated plates in Neurobasal-A medium with 2% B27, 1% GlutaMAX, and 100 U/mL penicillin–streptomycin (Catalog No. 17504044, 35050061, and 15140122, all from Thermo Fisher Scientific, USA) at 37 °C with 5% CO_2 [25,26]. All primary RGCs used in this study were authenticated by short tandem repeat (STR) profiling performed by Guangzhou Cellcook Biotech Co., Ltd. (Guangzhou, China) to confirm species origin and identity. The cells were routinely tested for mycoplasma contamination using the PCR-based Mycoplasma Detection Kit (Catalog No. C0301S, Beyotime, Shanghai, China), and all tests were negative before experimental use.

The *in vitro* study comprised two experimental designs (n = 6 per group):

(1) Validation of SIRT3 overexpression: AAV-NC: RGCs infected with AAV-NC for 48 h under a multiplicity of infection (MOI) set to 10; AAV-SIRT3: RGCs infected with AAV-SIRT3 under the same conditions.

(2) Functional study of the SIRT3/AMPK axis in NMDA-injured RGCs: (a) Control: Untreated RGCs maintained under normal culture conditions; (b) NMDA: RGCs received 100 µM N-methyl-D-aspartate (NMDA; Catalog No. M3262, Sigma-Aldrich, USA) for 24 h [26–28]; (c) NMDA + AAV-NC: RGCs infected with AAV-NC for 48 h (MOI 10), followed by NMDA exposure as above; (d) NMDA + AAV-SIRT3: RGCs infected with AAV-SIRT3 for 48 h (MOI 10), followed by NMDA exposure; (e) NMDA + AAV-SIRT3 + Compound C: RGCs infected with AAV-SIRT3 for 48 h, then treated with NMDA and Compound C (10 µM; Catalog No. 171261, MedChemExpress, USA) for 24 h [29].

2.3 Intraocular Pressure (IOP) Measurement

IOP of the right eye was recorded at weeks 0, 2, 4, and 6 using a rodent-specific rebound tonometer (TonoLab, Model: TV02, Icare Finland Oy, Finland). Rats were gently restrained without anesthesia, and measurements were taken between 9:00–11:00 AM to minimize circadian variation. For each eye, three averages readings (each from six readings) were obtained and the mean value was used for analysis.

2.4 Quantitative Real-Time PCR (qRT-PCR)

Total RNA was extracted from retinal tissues or cultured RGCs using TRIzol® reagent (Catalog No. 15596026, Invitrogen, Thermo Fisher Scientific, Waltham, MA, USA). Briefly, samples were homogenized in 1 mL TRIzol, mixed with 200 µL chloroform, centrifuged (12,000 ×g, 15 min, 4 °C), and the aqueous phase was precipitated with isopropanol, washed with 70% ethanol, and dissolved in RNase-free water. RNA purity and concentration were measured using a NanoDrop™ 2000 spectrophotometer (Model ND-2000, Thermo Fisher Scientific, USA). qRT-PCR was performed with the UniPeak U + One Step RT-qPCR SYBR Green Kit (Catalog No. UPT-

201, Guangzhou YuJia Biotechnology, Guangzhou, China) via a QuantStudio™ 6 Flex Real-Time instrument (Model: QS6 Flex, Applied Biosystems, Thermo Fisher Scientific, Waltham, MA, USA). Cycling conditions were as follows: reverse transcription at 55 °C, denaturation at 95 °C for 30 s, 40 amplification cycles (95 °C for 5 s, 60 °C for 30 s), ending in melting curve stage.

Primer sequences: SIRT3 forward 5′-GCTACATGCACGGTCTGTCGAA-3′, reverse 5′-CAATGTCGGGTTTCACAACGCC-3′; GAPDH forward 5′-ACTCCCTCAAGATTGTCAGC-3′, reverse 5′-AGTTGCTGTTGAAGTCACAGG-3′. Corresponding expression was adjusted to GAPDH using the $2^{-\Delta\Delta Ct}$ method.

2.5 Western Blot Analysis

Retinal tissues or cultured RGCs were homogenized in RIPA buffer (Beyotime, China) with protease and phosphatase inhibitors, and total protein levels were quantified via a BCA assay (Catalog No. 23225, Thermo Fisher, Waltham, MA, USA). Proteins (30 µg) were resolved by Sodium dodecyl sulfate–polyacrylamide gel electrophoresis (SDS-PAGE) and electroblotted onto PVDF membranes (Catalog No. IPVH00010, Millipore, Billerica, MA, USA).

The membranes were pretreated with 5% non-fat milk/TBST for 1 h at ambient temperature and exposed overnight at 4 °C to the following primary antibodies (all from Abcam, Cambridge, UK): SIRT3 (1:1000, ab118334), AMPK (1:1000, ab207442), phospho-AMPK (Thr172) (1:1000, ab133448), and β-actin (1:5000, ab8226). After washing, membranes underwent a 1-h incubation at ambient temperature with Horseradish peroxidase (HRP)-labeled goat anti-rabbit Immunoglobulin G (IgG) (1:5000, ab205718) or goat anti-mouse IgG (1:5000, ab205719) (both from Abcam). Protein bands were visualized using an enhanced chemiluminescence kit (Catalog No. 32106, Thermo Fisher Scientific, Waltham, MA, USA) and quantified by ImageJ software (Version 1.53t, NIH, Bethesda, MD, USA), normalized to β-actin.

2.6 Hematoxylin and Eosin (HE) Staining

At week 6, rats were euthanized under deep anesthesia by intraperitoneal injection of sodium barbiturate (150 mg/kg). Death was confirmed by the absence of heartbeat and respiration before tissue collection, in accordance with the American Veterinary Medical Association (AVMA) Guidelines for the Euthanasia of Animals (2020 edition). Eyes were enucleated, fixed in 4% paraformaldehyde for 24 h, dehydrated, embedded in paraffin, and sectioned at 5 µm thickness. Sections were stained with hematoxylin for 5 min and eosin for 2 min, dehydrated, cleared, and mounted. Retinal morphology was examined under a BX53 light microscope (Model BX53, Olympus Corporation, Tokyo, Japan), focusing on the ganglion and inner plexiform layers.

2.7 Terminal Deoxynucleotidyl Transferase dUTP Nick End Labeling (TUNEL) Assay

Paraffin-embedded retinal sections (5 µm) underwent deparaffinization, rehydration, and proteinase K treatment (20 µg/mL; Catalog No. 03115879001, Roche Diagnostics, Mannheim, Germany) for 15 minutes at room temperature. Following rinsing with PBS, slices were exposed to an *In Situ* Cell Death Detection Kit (Roche Diagnostics, Mannheim, Germany) for 1 hour at 37 °C in a humidified chamber, protected from light. DAPI (Catalog No. C1002, Beyotime, Shanghai, China) was applied to nuclei for 5 minutes. Images were acquired using a BX53 system, and TUNEL-positive cells were analyzed via ImageJ (Version 1.53t, NIH, Bethesda, MD, USA).

2.8 Cell Counting Kit-8 (CCK-8) Analysis

RGCs were plated in 96-well plates at an appropriate density and treated as indicated. At the end of treatment, 10 µL CCK-8 reagent (Catalog No. CK04, Dojindo Molecular Technologies, Kumamoto, Japan) was mixed with 100 µL medium per well and incubated for 2 h at 37 °C. Optical density (OD) at 450 nm was recorded with a SpectraMax iD3 microplate reader (Model iD3, Molecular Devices, San Jose, CA, USA). Viability was expressed as a ratio versus the control group.

2.9 Flow Cytometry Assay

After treatment, RGCs were collected, rinsed twice with cold PBS, and resuspended into 195 µL binding buffer. A total of 5 µL Annexin V-FITC and 10 µL propidium iodide (PI) (Catalog No. C1062 and C1052, both from Beyotime, Shanghai, China) were introduced, and the mixture was incubated for 15 min at room temperature in the dark. Samples were analyzed within 1 h using a flow cytometer (BD FACSCanto II, BD Biosciences, San Jose, CA, USA), and data were processed with FlowJo software (Version 10.8.1, Tree Star, Ashland, OR, USA) to determine the percentages of viable, early apoptotic, and late apoptotic/necrotic cells.

2.10 ROS Detection

ROS levels were quantified with DCFH-DA (Catalog No. S0033, Beyotime, Shanghai, China). For retinal tissue, eyes were collected at week 6, retinas were dissected on ice, homogenized in ice-cold PBS without phenol red (1 mM EDTA, Catalog No. AM9260G, Thermo Fisher Scientific, Waltham, MA, USA), and clarified by centrifugation (12,000 g, 10 min, 4 °C); protein content was quantified by BCA. Aliquots containing 50–100 µg protein in 100 µL underwent 30-min incubation with 10 µM DCFH-DA at 37 °C in darkness, and fluorescence measurement was read on a microplate reader. Signals were background-subtracted and normalized to protein, reported as RFU/µg protein.

For cultured RGCs, after treatments cells underwent 30-min loading with 10 µM DCFH-DA in serum-free

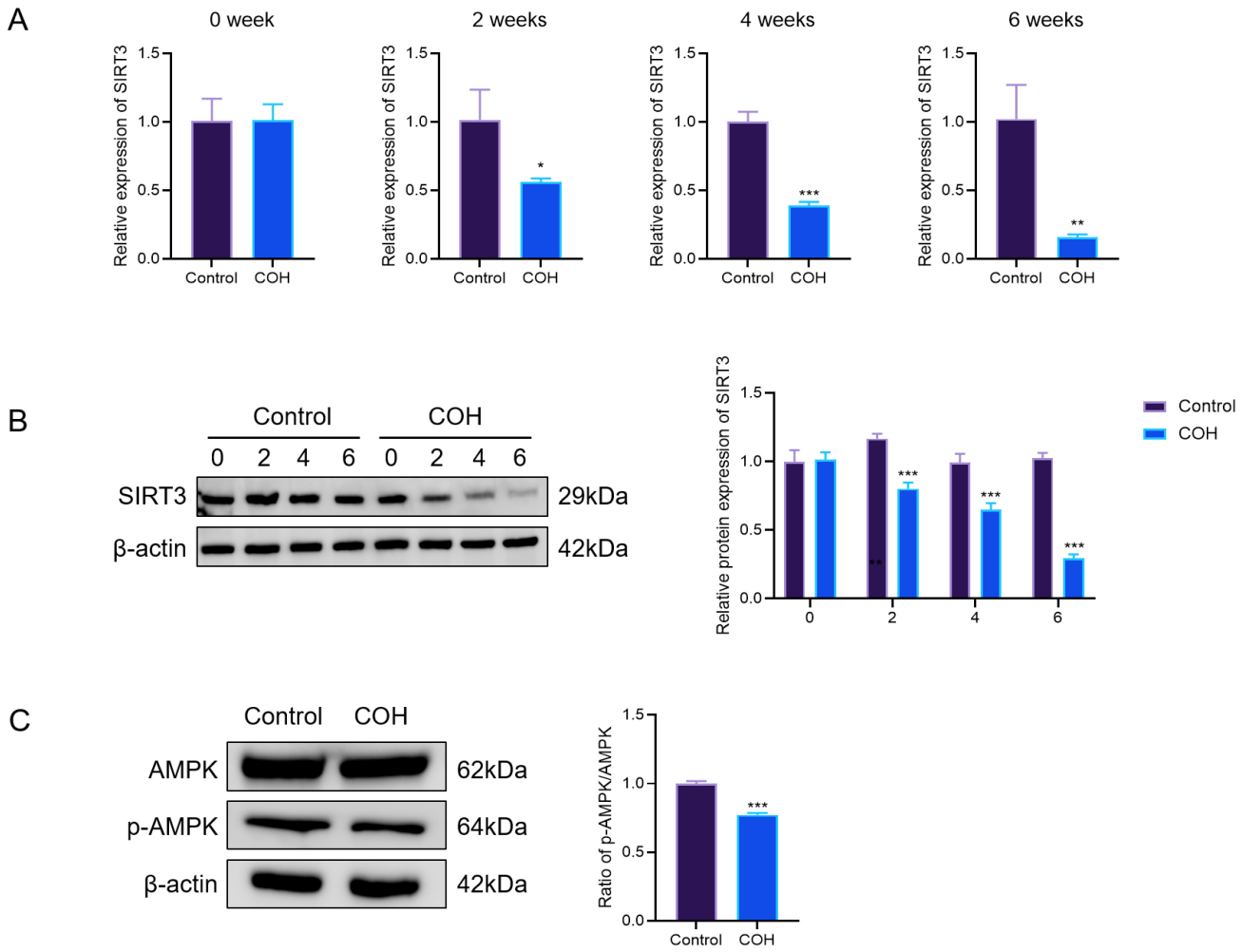

Fig. 1. Temporal changes of SIRT3 and AMPK phosphorylation in the COH model. (A) qRT-PCR analysis of retinal SIRT3 mRNA at 0, 2, 4, and 6 weeks. (B) Western blot analysis of SIRT3 protein over the same period. (C) Western blot analysis of AMPK and p-AMPK at week 6. Data were presented as mean ± SD (n = 6). *$p < 0.05$, **$p < 0.01$, ***$p < 0.001$ vs. Control group. SIRT3, Sirtuin 3; AMPK, AMP-activated protein kinase; COH, chronic ocular hypertension; qRT-PCR, Quantitative real-time PCR; SD, Sprague–Dawley.

medium at 37 °C under dark conditions, washed 3× with PBS, and imaged immediately without fixation on a fluorescence microscope (Model BX53, Olympus Corporation, Tokyo, Japan) using identical exposure/gain across groups. For quantification, five random non-overlapping fields/well were analyzed in ImageJ with a fixed threshold to obtain mean fluorescence intensity (MFI). Outcomes were standardized to the Control group and reported as percentage of Control.

2.11 Statistical Analysis

All statistics were conducted in SPSS 23.0 (IBM Corp., Armonk, NY, USA) and data are expressed as mean ± standard deviation (SD). Normality was assessed by the Shapiro–Wilk test. Differences between two groups were analyzed using the independent-samples *t*-test. For comparisons among multiple groups, one-way ANOVA followed by Tukey's post hoc test was used. For time-course measurements of IOP, two-way repeated-measures ANOVA with factors of group and time was applied, followed by Bonferroni correction for multiple comparisons. A $p < 0.05$ was considered statistically significant.

3. Results

3.1 SIRT3 Levels Decreases Over Time in the COH Model, Accompanied by Reduced AMPK Phosphorylation

To investigate the temporal dynamics in SIRT3 and AMPK signaling in glaucoma progression, we examined retinal tissues from the COH model at baseline (week 0) and at weeks 2, 4, and 6.

At the transcript level, qRT-PCR results showed no significant difference in retinal SIRT3 mRNA expression between Control and COH groups at week 0 ($p > 0.05$). From week 2 onward, SIRT3 mRNA in the COH group progressively declined, with reductions of approximately 40% at week 2 ($p < 0.05$), 65% at week 4 ($p < 0.001$), and 80% at week 6 ($p < 0.01$) compared with controls (Fig. 1A). Con-

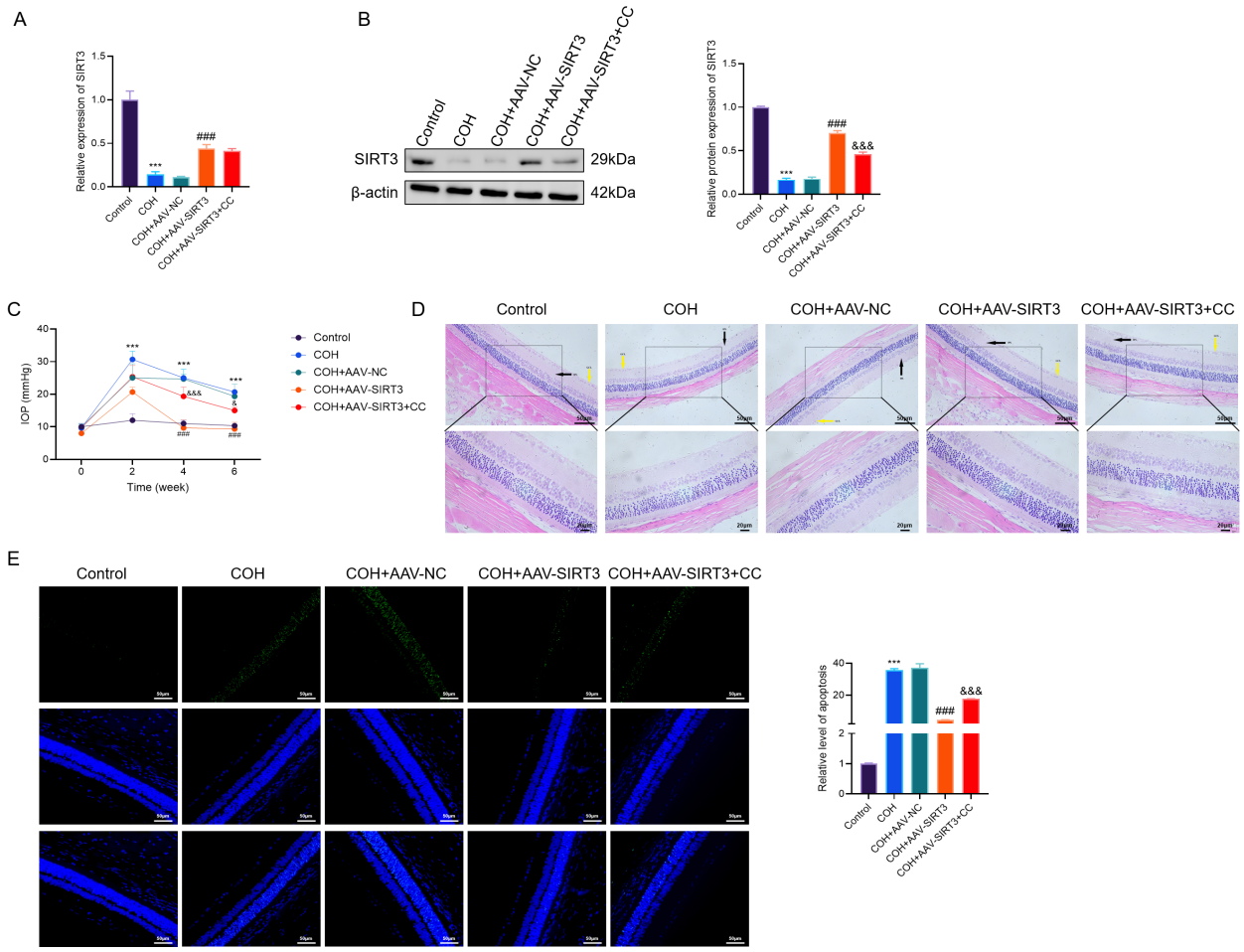

Fig. 2. Impact of SIRT3 upregulation on IOP, retinal morphology, as well as apoptosis in COH rats. (A) qRT-PCR analysis of retinal SIRT3 mRNA at week 6. (B) Immunoblotting with densitometric analysis of SIRT3 protein. (C) IOP at weeks 0, 2, 4, and 6. (D) HE staining of retinal sections, Black arrows indicate thinning/disruption of the ganglion cell layer (GCL), and yellow arrows indicate inner plexiform layer (IPL) degeneration. Upper panels: Scale bar = 50 µm; lower panels: Scale bar = 20 µm. (E) TUNEL staining showing apoptotic nuclei (green) and DAPI-labeled nuclei (blue), Scale bar = 50 µm. Values are presented as mean ± SD (n = 6). ***$p < 0.001$ vs. Control; $^{\#\#\#}p < 0.001$ vs. COH+AAV-NC; $^{\&}p < 0.05$, $^{\&\&\&}p < 0.001$ vs. COH+AAV-SIRT3. IOP, intraocular pressure; HE, hematoxylin and eosin; TUNEL, Terminal deoxynucleotidyl transferase dUTP nick end labeling; DAPI, 4′,6-diamidino-2-phenylindole; AAV, adeno-associated virus; NC, Negative control; CC, Compound C.

sistently, Western blot analysis revealed a gradual and sustained decrease in SIRT3 protein expression in COH retinas, showing significant reductions at weeks 2, 4, and 6 ($p < 0.001$) versus Control (Fig. 1B).

We next assessed AMPK signaling at week 6 (Fig. 1C). Total AMPK protein levels remained comparable between groups ($p > 0.05$), while phosphorylated AMPK (p-AMPK) was notably significantly reduced in the COH condition ($p < 0.001$), indicating suppressed AMPK activation under glaucomatous conditions.

Together, these results demonstrated a time-dependent downregulation of SIRT3 at both mRNA and protein expression in the COH model, which was accompanied by a corresponding reduction in AMPK phosphorylation at the later stages of disease progression.

3.2 Effects of SIRT3 Overexpression on IOP, Retinal Structure, and Apoptosis in COH Rats

To determine whether restoring SIRT3 expression confers neuroprotection *in vivo*, we first verified the efficiency of AAV-mediated SIRT3 overexpression. qRT-PCR showed that COH induction significantly decreased retinal SIRT3 mRNA compared with controls ($p < 0.001$; Fig. 2A). Delivery of AAV-SIRT3 markedly restored SIRT3 transcript levels ($p < 0.001$), whereas co-administration of Compound C produced a modest but not marked reduction in SIRT3 levels. Western blotting revealed a consistent trend at the protein level ($p < 0.001$; Fig. 2B).

Functionally, COH induction caused a pronounced elevation in IOP from week 2 onward, peaking at week 2 and remaining significantly higher than baseline through week 6

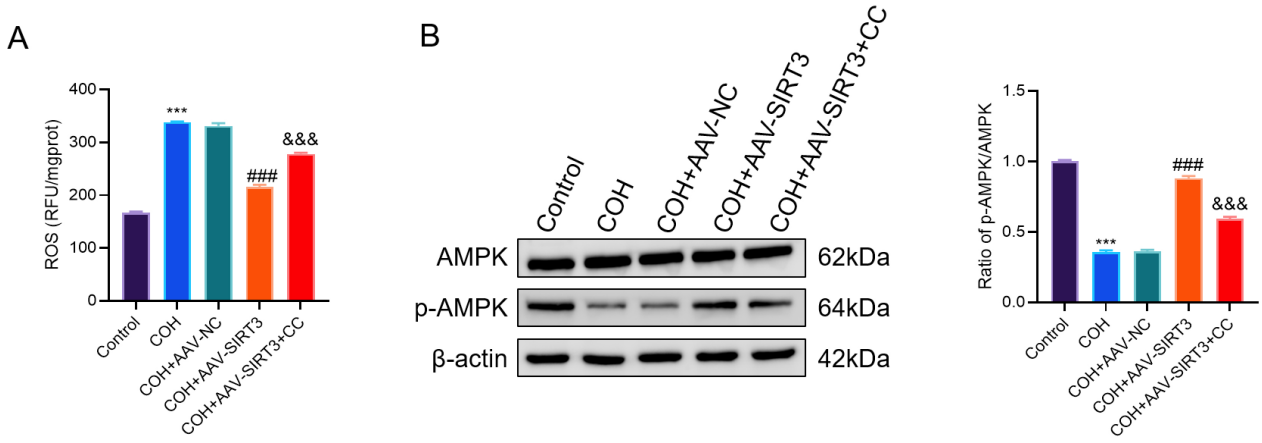

Fig. 3. SIRT3 attenuates retinal oxidative stress and promotes AMPK activation in COH rats. (A) Retinal ROS levels in each group. (B) Immunoblotting with densitometric analysis of total AMPK, phosphorylated AMPK (p-AMPK), and their ratio. Results are reported as mean ± SD (n = 6). ***$p < 0.001$ vs. Control; $^{###}p < 0.001$ vs. COH+AAV-NC; $^{\&\&\&}p < 0.001$ vs. COH+AAV-SIRT3.

($p < 0.001$). SIRT3 overexpression substantially attenuated this increase ($p < 0.001$), while Compound C co-treatment partly counteracted the reduction ($p < 0.05$) (Fig. 2C).

Histological assessment at week 6 revealed marked retinal thinning and disruption of the ganglion cell layer (GCL) and inner plexiform layer (IPL) in COH and COH+AAV-NC groups. In contrast, SIRT3 overexpression preserved overall retinal architecture, with denser GCLs and more intact IPL. This protective effect was notably diminished in the presence of Compound C (Fig. 2D).

In line with the morphological findings, TUNEL staining showed abundant apoptotic cells in COH and COH+AAV-NC groups ($p < 0.01$). SIRT3 overexpression significantly reduced retinal apoptosis ($p < 0.01$), whereas Compound C co-treatment diminished this anti-apoptotic effect ($p < 0.001$) (Fig. 2E).

Taken together, the findings demonstrated that SIRT3 overexpression alleviated IOP elevation, preserved retinal structural integrity, and inhibited apoptosis in COH rats. These neuroprotective effects appear to be at least partially dependent on AMPK activation.

3.3 SIRT3 Attenuates Retinal Oxidative Stress and Induces AMPK Activation Within COH Rats

To determine whether SIRT3 regulates oxidative stress in the glaucomatous retina and to evaluate the potential involvement of AMPK signaling pathway, we measured retinal ROS levels and AMPK phosphorylation in COH rats with or without SIRT3 overexpression and AMPK inhibition.

ROS detection showed that retinal ROS levels were significantly elevated in the COH and COH+AAV-NC groups compared with the Control group ($p < 0.001$). Overexpression of SIRT3 markedly reduced ROS accumulation ($p < 0.001$), whereas Compound C co-treatment weakened this effect ($p < 0.001$) (Fig. 3A).

Immunoblotting showed no significant change in total AMPK protein levels across groups ($p > 0.05$). However, phosphorylated AMPK expression was significantly decreased in COH rats compared with Controls ($p < 0.001$), restored by SIRT3 overexpression ($p < 0.001$), and partially suppressed again by Compound C treatment ($p < 0.001$) (Fig. 3B).

Taken together, these results indicate that SIRT3 alleviates oxidative stress in the glaucomatous retina, at least in part, through activation of the AMPK signaling pathway.

3.4 SIRT3 Overexpression Protects RGCs From NMDA-Induced Cytotoxicity and Apoptosis via AMPK Signaling

To further validate the neuroprotective role of SIRT3 observed *in vivo*, we established an *in vitro* NMDA-induced injury model using primary RGCs.

qRT-PCR confirmed the efficiency of AAV-mediated SIRT3 overexpression, showing significantly elevated SIRT3 mRNA levels in the AAV-SIRT3 group compared with the AAV-NC group ($p < 0.001$; Fig. 4A). Exposure to NMDA markedly suppressed endogenous SIRT3 expression in RGCs ($p < 0.001$), which was restored by AAV-SIRT3 transduction ($p < 0.01$). Co-treatment with Compound C moderately reduced this restoration, suggesting the involvement of AMPK signaling (Fig. 4B).

Functionally, the CCK-8 cell viability assay revealed that NMDA exposure significantly decreased RGC viability ($p < 0.001$). SIRT3 overexpression markedly enhanced cell viability ($p < 0.001$), whereas Compound C treatment significantly reduced this protective effect ($p < 0.001$) (Fig. 4C).

Flow cytometry showed that NMDA exposure substantially increased the apoptotic rate of RGCs ($p < 0.001$). Overexpression of SIRT3 significantly reduced apoptosis ($p < 0.001$), while Compound C co-treatment partially reversed this anti-apoptotic effect ($p < 0.01$) (Fig. 4D).

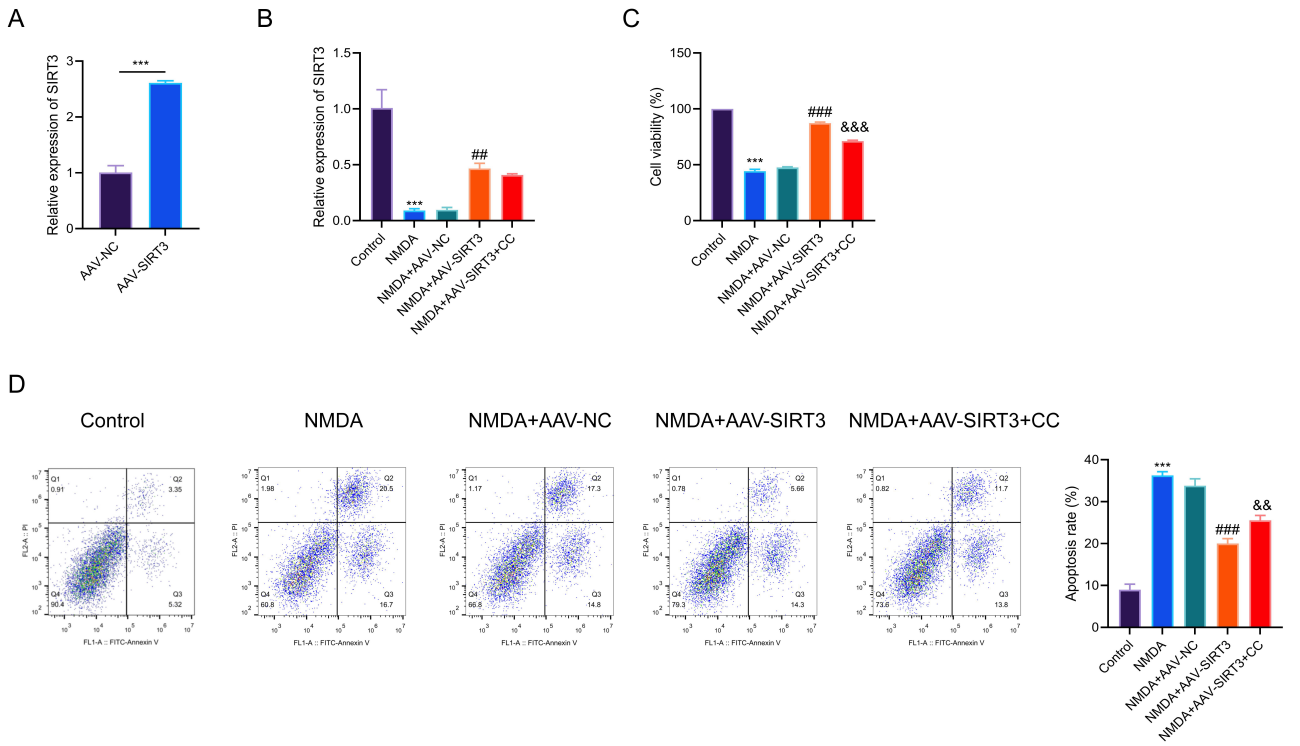

Fig. 4. Effects of SIRT3 overexpression on NMDA-induced cytotoxicity and apoptosis in RGCs via AMPK signaling. (A) qRT-PCR validation of SIRT3 overexpression in RGCs. (B) SIRT3 mRNA levels in NMDA-injured RGCs under different treatments. (C) Cell viability measured by CCK-8 assay. (D) Flow cytometry analysis and quantification of apoptosis rates. Data were expressed as mean ± SD (n = 3). ***$p < 0.001$ vs. Control; $^{\#\#}p < 0.01$, $^{\#\#\#}p < 0.001$ vs. NMDA + AAV-NC; $^{\&\&}p < 0.01$, $^{\&\&\&}p < 0.001$ vs. NMDA + AAV-SIRT3. NMDA, N-methyl-D-aspartate; RGCs, retinal ganglion cells; CCK-8, Cell Counting Kit-8.

Collectively, these results demonstrate that SIRT3 mitigates NMDA-induced RGC injury by enhancing cell survival and suppressing apoptosis, and that these protective effects are at least partially mediated through AMPK activation.

3.5 SIRT3 Regulates ROS Levels in NMDA-Injured RGCs via AMPK Signaling

Given that the *in vivo* results suggested that SIRT3 modulates oxidative stress through AMPK signaling, we further investigated intracellular ROS changes in NMDA-injured RGCs. ROS immunofluorescence staining revealed a marked increase in ROS signals following NMDA exposure ($p < 0.001$). AAV-mediated SIRT3 overexpression significantly reduced ROS accumulation, whereas co-treatment with the AMPK inhibitor Compound C partially abolished this reduction ($p < 0.01$) (Fig. 5A).

Immunoblot analysis showed no significant difference in total AMPK protein expression among the groups. However, NMDA exposure significantly decreased the p-AMPK/AMPK ratio ($p < 0.001$), which was restored by SIRT3 overexpression and suppressed again by Compound C co-treatment ($p < 0.001$) (Fig. 5B).

Collectively, these findings demonstrate that SIRT3 effectively mitigates NMDA-induced oxidative stress in RGCs by activating the AMPK pathway, whereas AMPK inhibition markedly attenuates this protective effect, underscoring the critical role of the SIRT3/AMPK axis in regulating oxidative stress.

4 Discussion

Although reducing intraocular pressure (IOP) remains the cornerstone of glaucoma management, a subset of patients continues to experience progressive vision loss despite well-controlled IOP, suggesting the involvement of IOP-independent neurodegenerative mechanisms. Using a chronic ocular hypertension (COH) rat model and an *in vitro* NMDA-induced retinal ganglion cell (RGC) injury model, this study systematically investigated the role of the SIRT3/AMPK signaling axis in glaucoma-related neuroprotection. We found that SIRT3 expression was persistently downregulated in the COH model, accompanied by reduced AMPK phosphorylation. Overexpression of SIRT3 lowered IOP, preserved retinal morphology, decreased oxidative stress, and inhibited apoptosis, whereas these protective effects were partially reversed by the AMPK inhibitor Compound C. Collectively, our findings suggest that SIRT3 and its downstream AMPK signaling constitute a critical regulatory axis in neuroprotection against glaucomatous injury.

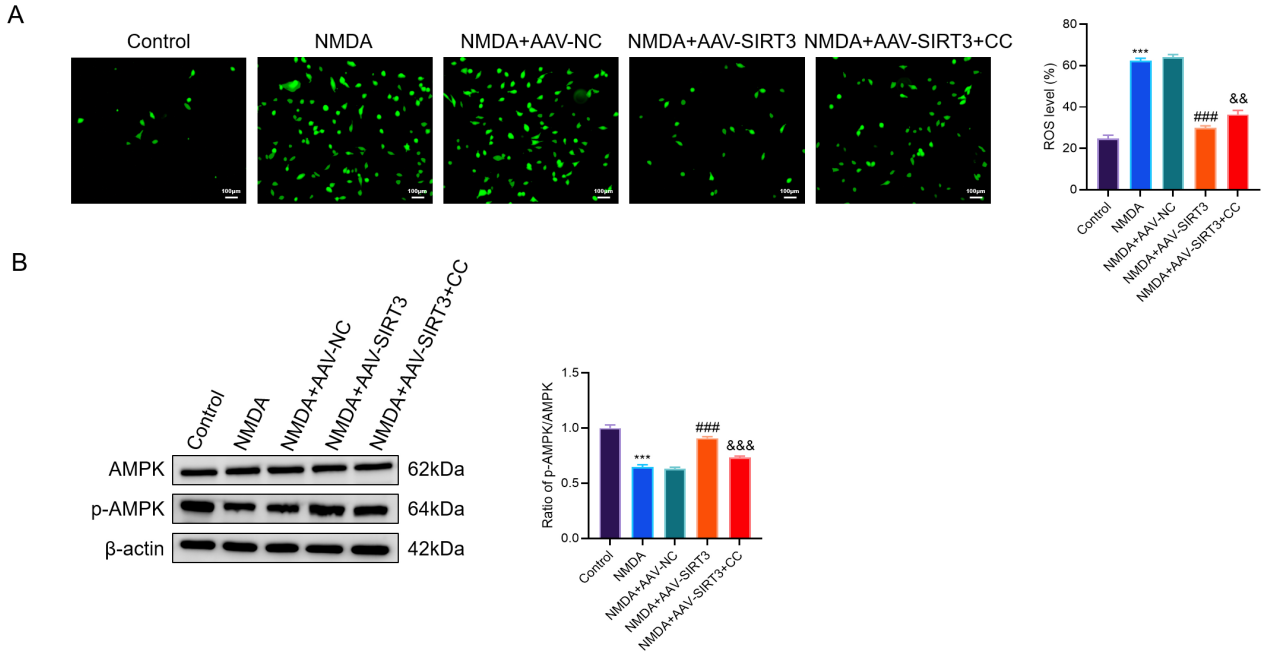

Fig. 5. SIRT3 reduces ROS in NMDA-injured RGCs via AMPK. (A) ROS immunofluorescence (green) and quantification. Scale bar = 100 μm. (B) Western blot of AMPK and p-AMPK, with p-AMPK/AMPK ratio. Data were expressed as mean ± SD (n = 3). ***$p < 0.001$ vs. Control; $^{\#\#\#}p < 0.001$ vs. NMDA + AAV-NC; $^{\&\&}p < 0.01$, $^{\&\&\&}p < 0.001$ vs. NMDA + AAV-SIRT3.

The observed progressive reduction of SIRT3 expression and AMPK phosphorylation in the COH model suggests early mitochondrial dysfunction and impaired cellular energy homeostasis during glaucoma progression. Similar SIRT3 downregulation has been reported in other neurodegenerative and ischemic models, where mitochondrial stress and oxidative damage suppress SIRT3 transcription and deacetylase activity [30]. Reduced AMPK activation may further exacerbate this process by limiting PGC-1α–mediated mitochondrial biogenesis and antioxidant responses, leading to cumulative mitochondrial damage and enhanced vulnerability of retinal ganglion cells [31]. These findings indicate that loss of the SIRT3–AMPK signaling cascade could represent an early molecular event contributing to RGC degeneration in chronic ocular hypertension.

At the molecular level, SIRT3, a mitochondrial NAD^+-dependent deacetylase, has been reported to protect against various neurodegenerative disorders by regulating mitochondrial bioenergetics, antioxidant defense, and apoptosis-related pathways [9]. In the present study, the sustained downregulation of SIRT3 in the COH model correlated with increased oxidative stress, and SIRT3 overexpression significantly reduced ROS accumulation, suggesting that its neuroprotective role may involve enhancement of mitochondrial antioxidant capacity, potentially through deacetylation and activation of manganese superoxide dismutase (MnSOD). AMPK, a central energy sensor, promotes antioxidant defense under metabolic stress by activating the Nrf2 and PGC-1α pathways [32]. The restoration of p-AMPK levels following SIRT3 overexpression, and their partial suppression by Compound C, supports a mediating role of AMPK in this process. However, we cannot exclude the possibility that SIRT3 also exert neuroprotection through AMPK-independent mechanisms, such as modulation of Bcl-2 family proteins or activation of mitophagy.

From a functional perspective, RGCs represent one of the most vulnerable neuronal populations in the retina, and their survival is essential for visual signal transmission [33]. We observed that SIRT3 overexpression not only ameliorated retinal structural damage in COH rats but also improved cell viability and reduced apoptosis in NMDA-injured RGCs. These findings indicate that SIRT3 exerts broad-spectrum neuroprotection in both chronic and acute injury models. Although chronic IOP elevation and acute NMDA excitotoxicity differ in etiology and time course [34], both share common pathological pathways, including oxidative stress, mitochondrial dysfunction, and apoptotic signaling, which may explain the consistent neuroprotective effects of SIRT3 observed across models.

Regarding the SIRT3/AMPK signaling axis, our results align with previous reports in other neurological disease models, including ischemic brain injury and Alzheimer's disease, where SIRT3-mediated activation of AMPK reduced oxidative damage and neuronal loss [35, 36]. The novelty of this study lies in the first integrated *in vivo* and *in vitro* demonstration of SIRT3/AMPK-dependent neuroprotection in glaucoma, complemented by pharmacological inhibition experiments that verify the partial dependence on AMPK activation. Nonetheless, AMPK activa-

tion is context-dependent, and its prolonged stimulation under glaucomatous conditions may exert dual effects; therefore, further research is required to delineate the threshold and duration of AMPK activation that confer optimal neuroprotection.

In conclusion, this study provides the first comprehensive evidence from both *in vivo* and *in vitro* models that SIRT3 confers neuroprotection against glaucoma-associated injury, primarily through AMPK pathway activation. These findings advance our understanding of IOP-independent mechanisms in glaucoma pathogenesis and highlight the SIRT3/AMPK axis as a promising therapeutic target for neuroprotective intervention.

Study Limitations

This study has several limitations. First, although six animals were included per group, the overall sample size remains relatively small and may limit statistical robustness; thus, power analysis–based sample size estimation should be incorporated in future studies. Second, while the COH and NMDA models are complementary, neither fully replicates the multifactorial pathophysiology of glaucoma. Incorporating genetic models (e.g., DBA/2J mice), aged animals, and longitudinal visual function assessments such as pattern electroretinography (PERG) or optokinetic tracking would enhance translational relevance. Third, our mechanistic insights were primarily derived from AAV-mediated overexpression and the use of Compound C, which is not entirely specific for AMPK inhibition. Future studies employing genetic knockdown or knockout approaches, coupled with assessment of downstream AMPK targets (e.g., phosphorylated ACC, PGC-1α), would provide more definitive evidence. Fourth, because SIRT3 overexpression also lowered IOP in the COH model, part of its neuroprotective effect may relate to IOP reduction rather than direct signaling; thus, IOP-matched controls or statistical adjustment for cumulative IOP exposure are warranted in future work. Finally, this study mainly focused on structural and molecular endpoints, lacking functional assessments of the visual pathway. Integrating electrophysiological and multi-omics analyses in subsequent studies will offer a more comprehensive understanding of the SIRT3/AMPK axis in glaucoma.

5. Conclusion

This study provides clear evidence that SIRT3 exerts potent neuroprotective effects in glaucoma-associated injury, primarily through activation of the AMPK signaling pathway. Using both a chronic ocular hypertension (COH) rat model and an *in vitro* NMDA-induced retinal ganglion cell (RGC) injury model, we demonstrated that SIRT3 overexpression alleviates oxidative stress, preserves retinal architecture, and inhibits apoptosis, whereas AMPK inhibition partially counteracts these protective effects. Collectively, these findings identify the SIRT3/AMPK signaling axis as a promising therapeutic target for neuroprotection in glaucoma. Future studies should integrate genetic models, functional visual assessments, and optimized pharmacological interventions to further elucidate the temporal dynamics and downstream effectors of this pathway. Such work will facilitate translational advances toward the development of mechanism-based, multimodal therapeutic strategies for glaucoma management.

Availability of Data and Materials

The datasets used and analyzed during the current study are available from the corresponding author on reasonable request.

Author Contributions

All authors contributed to the study conception and design. Material preparation, data collection and analysis were performed by YY and XXC. The first draft of this manuscript was written by FC and XHL and all authors commented on previous versions of the manuscript. All authors read and approved the final manuscript. All authors have participated sufficiently in the work and agreed to be accountable for all aspects of the work.

Ethics Approval and Consent to Participate

All animal experiments were conducted in accordance with the guidelines for the care and use of laboratory animals and approved by the Ethics Committee of Guangzhou Medical University (Approval No.: KTDW-2024-00947). Every effort was made to minimize animal suffering and to reduce the number of animals used in this study.

Acknowledgment

Not applicable.

Funding

This research received no external funding.

Conflict of Interest

The authors declare no conflict of interest.

Declaration of AI and AI-Assisted Technologies in the Writing Process

During the preparation of this work, the authors used ChatGPT (OpenAI, USA) to check spelling and grammar. After using this tool, the authors reviewed and edited the content as needed and take full responsibility for the content of the publication.

Supplementary Material

Supplementary material associated with this article can be found, in the online version, at https://doi.org/10.31083/FBL46525.

References

[1] Foster PJ, Khawaja A, Balk LJ, Muthy Z, Petzold A. Sensory loss—vision. In Brayne C, Feigin VL, Launer LJ, Logroscino G (eds.) Oxford Textbook of Neurologic and Neuropsychiatric Epidemiology (pp. 345–354). Oxford University Press: Oxford, UK. 2020. https://doi.org/10.1093/med/9780198749493.003.0033.

[2] Bouckaert L. NON-VIRAL/VIRAL STRATEGY AT THE LEVEL OF THE ANTERIOR SEGMENT FOR THE TREATMENT OF GLAUCOMA [master's thesis]. Belgium: Ghent University. 2021.

[3] Alves FS, Duarte S, Cabrita A, Marques C, Oliveira A, Machado M, *et al*. Nanotechnology Devices for Glaucoma Surgical Treatment: A Systematic Review. 2023. https://doi.org/10.20944/preprints202309.1935.v1. (preprint)

[4] Nita M, Grzybowski A. The Role of the Reactive Oxygen Species and Oxidative Stress in the Pathomechanism of the Age-Related Ocular Diseases and Other Pathologies of the Anterior and Posterior Eye Segments in Adults. Oxidative Medicine and Cellular Longevity. 2016; 2016: 3164734. https://doi.org/10.1155/2016/3164734.

[5] Inman DM, Harun-Or-Rashid M. Metabolic Vulnerability in the Neurodegenerative Disease Glaucoma. Frontiers in Neuroscience. 2017; 11: 146. https://doi.org/10.3389/fnins.2017.00146.

[6] Cheung W, Guo L, Cordeiro MF. Neuroprotection in glaucoma: drug-based approaches. Optometry and Vision Science: Official Publication of the American Academy of Optometry. 2008; 85: 406–416. https://doi.org/10.1097/OPX.0b013e31817841e5.

[7] Hurley DJ, Normile C, Irnaten M, O'Brien C. The Intertwined Roles of Oxidative Stress and Endoplasmic Reticulum Stress in Glaucoma. Antioxidants (Basel, Switzerland). 2022; 11: 886. https://doi.org/10.3390/antiox11050886.

[8] Khan H, Tiwari P, Kaur A, Singh TG. Sirtuin Acetylation and Deacetylation: a Complex Paradigm in Neurodegenerative Disease. Molecular Neurobiology. 2021; 58: 3903–3917. https://doi.org/10.1007/s12035-021-02387-w.

[9] Tyagi A, Pugazhenthi S. A Promising Strategy to Treat Neurodegenerative Diseases by SIRT3 Activation. International Journal of Molecular Sciences. 2023; 24: 1615. https://doi.org/10.3390/ijms24021615.

[10] Kandy AT, Chand J, Baba MZ, Subramanian G. Is SIRT3 and Mitochondria a Reliable Target for Parkinson's Disease and Aging? A Narrative Review. Molecular Neurobiology. 2025; 62: 6898–6912. https://doi.org/10.1007/s12035-024-04486-w.

[11] Gleave JA, Arathoon LR, Trinh D, Lizal KE, Giguère N, Barber JHM, *et al*. Sirtuin 3 rescues neurons through the stabilisation of mitochondrial biogenetics in the virally-expressing mutant α-synuclein rat model of parkinsonism. Neurobiology of Disease. 2017; 106: 133–146. https://doi.org/10.1016/j.nbd.2017.06.009.

[12] Zhang J, Xiang H, Liu J, Chen Y, He RR, Liu B. Mitochondrial Sirtuin 3: New emerging biological function and therapeutic target. Theranostics. 2020; 10: 8315–8342. https://doi.org/10.7150/thno.45922.

[13] Trinh D, Al Halabi L, Brar H, Kametani M, Nash JE. The role of SIRT3 in homeostasis and cellular health. Frontiers in Cellular Neuroscience. 2024; 18: 1434459. https://doi.org/10.3389/fncel.2024.1434459.

[14] Jang KH, Hwang Y, Kim E. PARP1 Impedes SIRT1-Mediated Autophagy during Degeneration of the Retinal Pigment Epithelium under Oxidative Stress. Molecules and Cells. 2020; 43: 632–644. https://doi.org/10.14348/molcells.2020.0078.

[15] Cheng J, Keuthan CJ, Esumi N. The many faces of SIRT6 in the retina and retinal pigment epithelium. Frontiers in Cell and Developmental Biology. 2023; 11: 1244765. https://doi.org/10.3389/fcell.2023.1244765.

[16] Giralt A, Villarroya F. SIRT3, a pivotal actor in mitochondrial functions: metabolism, cell death and aging. The Biochemical Journal. 2012; 444: 1–10. https://doi.org/10.1042/BJ20120030.

[17] He J, Liu X, Su C, Wu F, Sun J, Zhang J, *et al*. Inhibition of Mitochondrial Oxidative Damage Improves Reendothelialization Capacity of Endothelial Progenitor Cells via SIRT3 (Sirtuin 3)-Enhanced SOD2 (Superoxide Dismutase 2) Deacetylation in Hypertension. Arteriosclerosis, Thrombosis, and Vascular Biology. 2019; 39: 1682–1698. https://doi.org/10.1161/ATVBAHA.119.312613.

[18] Han L, Li J, Li J, Pan C, Xiao Y, Lan X, *et al*. Activation of AMPK/Sirt3 pathway by phloretin reduces mitochondrial ROS in vascular endothelium by increasing the activity of MnSOD via deacetylation. Food & Function. 2020; 11: 3073–3083. https://doi.org/10.1039/c9fo02334h.

[19] Herskovits AZ, Guarente L. Sirtuin deacetylases in neurodegenerative diseases of aging. Cell Research. 2013; 23: 746–758. https://doi.org/10.1038/cr.2013.70.

[20] Baur JA, Sinclair DA. Therapeutic potential of resveratrol: the *in vivo* evidence. Nature Reviews. Drug Discovery. 2006; 5: 493–506. https://doi.org/10.1038/nrd2060.

[21] Shukal DK, Malaviya PB, Sharma T. Role of the AMPK signalling pathway in the aetiopathogenesis of ocular diseases. Human & Experimental Toxicology. 2022; 41: 9603271211063165. https://doi.org/10.1177/09603271211063165.

[22] Chang KC, Liu PF, Chang CH, Lin YC, Chen YJ, Shu CW. The interplay of autophagy and oxidative stress in the pathogenesis and therapy of retinal degenerative diseases. Cell & Bioscience. 2022; 12: 1. https://doi.org/10.1186/s13578-021-00736-9.

[23] Huang S, Huang P, Liu X, Lin Z, Wang J, Xu S, *et al*. Relevant variations and neuroprotecive effect of hydrogen sulfide in a rat glaucoma model. Neuroscience. 2017; 341: 27–41. https://doi.org/10.1016/j.neuroscience.2016.11.019.

[24] Yu H, Zhong H, Li N, Chen K, Chen J, Sun J, *et al*. Osteopontin activates retinal microglia causing retinal ganglion cells loss via p38 MAPK signaling pathway in glaucoma. FASEB Journal: Official Publication of the Federation of American Societies for Experimental Biology. 2021; 35: e21405. https://doi.org/10.1096/fj.202002218R.

[25] Hu X, Dai Y, Sun X. Parkin overexpression protects retinal ganglion cells against glutamate excitotoxicity. Molecular Vision. 2017; 23: 447–456.

[26] Amina M, Bhat RS, Al-Dbass AM, Musayeib NM, Fahmy R, Alhadlaq L, *et al*. The protective effect of *Moringa oleifera* plant extract against glutamate-induced DNA damage and reduced cell viability in a primary retinal ganglion cell line. PeerJ. 2021; 9: e11569. https://doi.org/10.7717/peerj.11569.

[27] Dai Y, Hu X, Sun X. Overexpression of parkin protects retinal ganglion cells in experimental glaucoma. Cell Death & Disease. 2018; 9: 88. https://doi.org/10.1038/s41419-017-0146-9.

[28] Sühs KW, Fairless R, Williams SK, Heine K, Cavalié A, Diem R. N-methyl-D-aspartate receptor blockade is neuroprotective in experimental autoimmune optic neuritis. Journal of Neuropathology & Experimental Neurology. 2014; 73: 507–518. https://doi.org/10.1097/nen.0000000000000073.

[29] Zhang K, Wang T, Sun GF, Xiao JX, Jiang LP, Tou FF, *et al*. Metformin protects against retinal ischemia/reperfusion injury through AMPK-mediated mitochondrial fusion. Free Radical Biology & Medicine. 2023; 205: 47–61. https://doi.org/10.1016/j.freeradbiomed.2023.05.019.

[30] Li H, Cai Z. SIRT3 regulates mitochondrial biogenesis in aging-related diseases. Journal of Biomedical Research. 2022; 37: 77–88. https://doi.org/10.7555/JBR.36.20220078.

[31] Guo X, Jiang Q, Tuccitto A, Chan D, Alqawlaq S, Won GJ, *et*

al. The AMPK-PGC-1α signaling axis regulates the astrocyte glutathione system to protect against oxidative and metabolic injury. Neurobiology of Disease. 2018; 113: 59–69. https://doi.org/10.1016/j.nbd.2018.02.004.

[32] Rius-Pérez S, Torres-Cuevas I, Millán I, Ortega ÁL, Pérez S. PGC-1α, Inflammation, and Oxidative Stress: An Integrative View in Metabolism. Oxidative Medicine and Cellular Longevity. 2020; 2020: 1452696. https://doi.org/10.1155/2020/1452696.

[33] Sanes JR, Masland RH. The types of retinal ganglion cells: current status and implications for neuronal classification. Annual Review of Neuroscience. 2015; 38: 221–246. https://doi.org/10.1146/annurev-neuro-071714-034120.

[34] Osborne NN, Casson RJ, Wood JPM, Chidlow G, Graham M, Melena J. Retinal ischemia: mechanisms of damage and potential therapeutic strategies. Progress in Retinal and Eye Research. 2004; 23: 91–147. https://doi.org/10.1016/j.preteyeres.2003.12.001.

[35] Liu Y, Cheng A, Li YJ, Yang Y, Kishimoto Y, Zhang S, *et al*. SIRT3 mediates hippocampal synaptic adaptations to intermittent fasting and ameliorates deficits in APP mutant mice. Nature Communications. 2019; 10: 1886. https://doi.org/10.1038/s41467-019-09897-1.

[36] Wan R, Fan J, Song H, Sun W, Yin Y. Oxygen-Glucose Deprivation/Reperfusion-Induced Sirt3 Reduction Facilitated Neuronal Injuries in an Apoptosis-Dependent Manner During Prolonged Reperfusion. Neurochemical Research. 2022; 47: 1012–1024. https://doi.org/10.1007/s11064-021-03502-y.